Gault et al., http://www.jcb.org/cgi/content/full/jcb.201408049/DC1

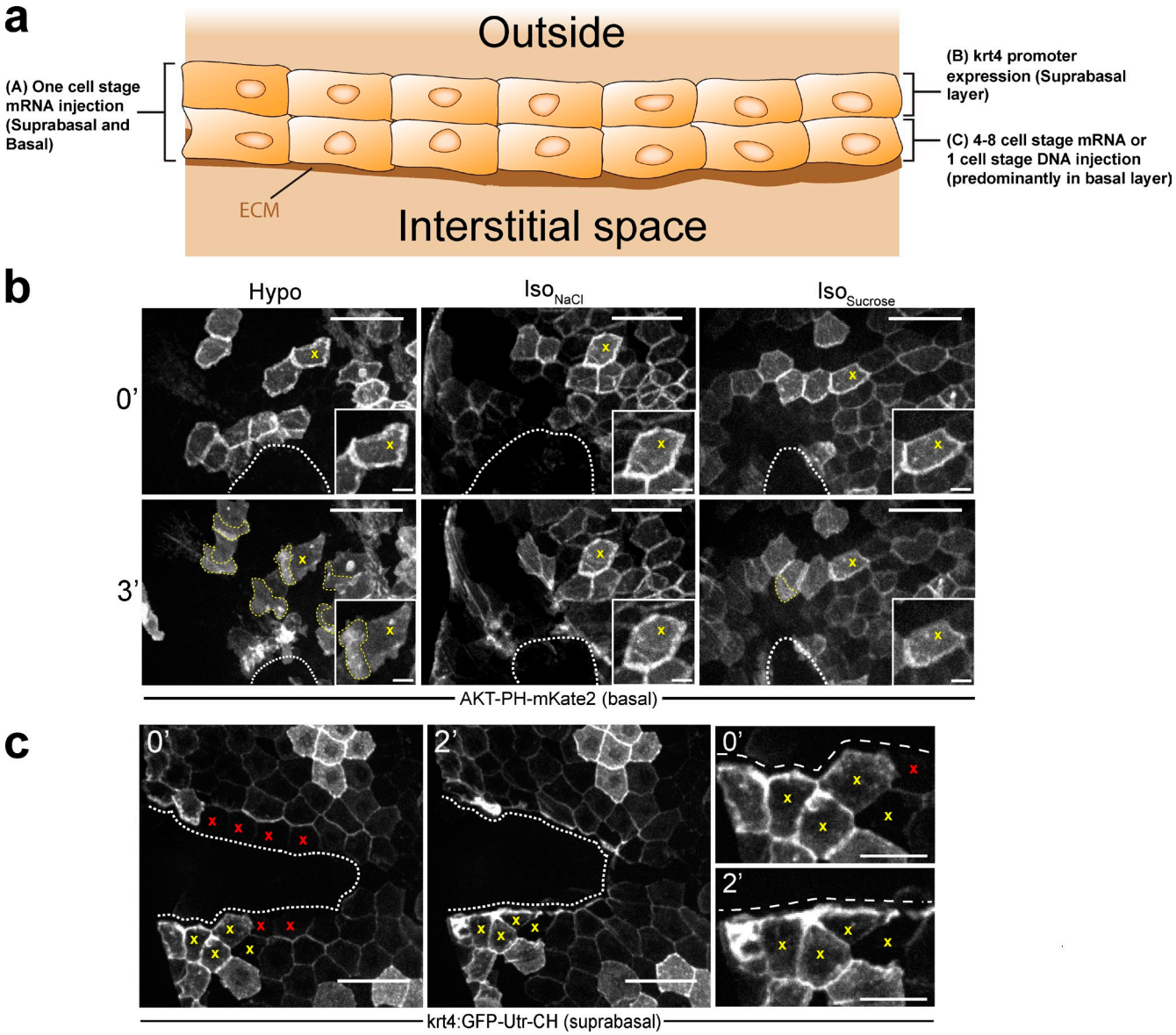

Figure S1. **Labeling distinct epidermal cell populations reveals that basal epidermal cells migrate beneath the suprabasal cell layer in response to decreased osmotic pressure.** (a) Schematic representation of the larval zebrafish tail fin epidermis at 3 dpf, highlighting the epithelial labeling methodology performed. (a, A) One-cell-stage embryonic mRNA injection (yolk sac) permits labeling of both epidermal layers. (a, B) Stable transgenic or transient expression driven by the *krt4* promoter results in fluorescent marker expression in the suprabasal (surface) layer exclusively. (a, C) mRNA injection into yolk of 4–8-cell embryos, or DNA plasmid injection into one-cell-stage embryos, followed by epifluorescence selection, labels predominantly basal epidermal cells in a mosaic pattern. (b and c) Time-lapse images of representative 2.5–3-dpf zebrafish larvae at the indicated times after UV laser–induced injury. (b) Mosaically labeled AKT-PH-mKate2 larvae puncture wounded in either hypotonic (hypo) or isotonic (Iso_{NaCl} or $Iso_{Sucrose}$) E3 medium (white broken line, wound margin). (b, left) Wounding in hypotonic E3 medium revealed propagated lamellipodia formation (yellow broken lines) and translocation toward the wound. (b, center) Wounding in Iso_{NaCl} failed to induce noticeable protrusions. (b, right) Wounding in $Iso_{Sucrose}$ exhibited small or sporadic lamellipodia in basal cells usually closer to the wound (yellow dotted lines), whereas lamellipodia formation in more distal regions was inhibited. Yellow x, representative morphological features of cells at comparable distances from the wound margin in the hypotonic and isotonic treatments. (c) Cut-wounded larva injected with *krt4*:GFP-UtrCH DNA for transient expression in the suprabasal epidermal layer. Actin becomes enriched on cell sides facing the wound (white broken line). At the same time, cells form a smooth wound margin (compare yellow x in 0′ and 2′ and magnifications [right]). Note that some margin cells present at time 0′ (red x's) are extruded from the tissue by 2′. Bars: (b, main panels) 50 µm; (b, insets) 10 µm; (c, two left panels) 50 µm; (c, enlarged panels on the right) 25 µm.

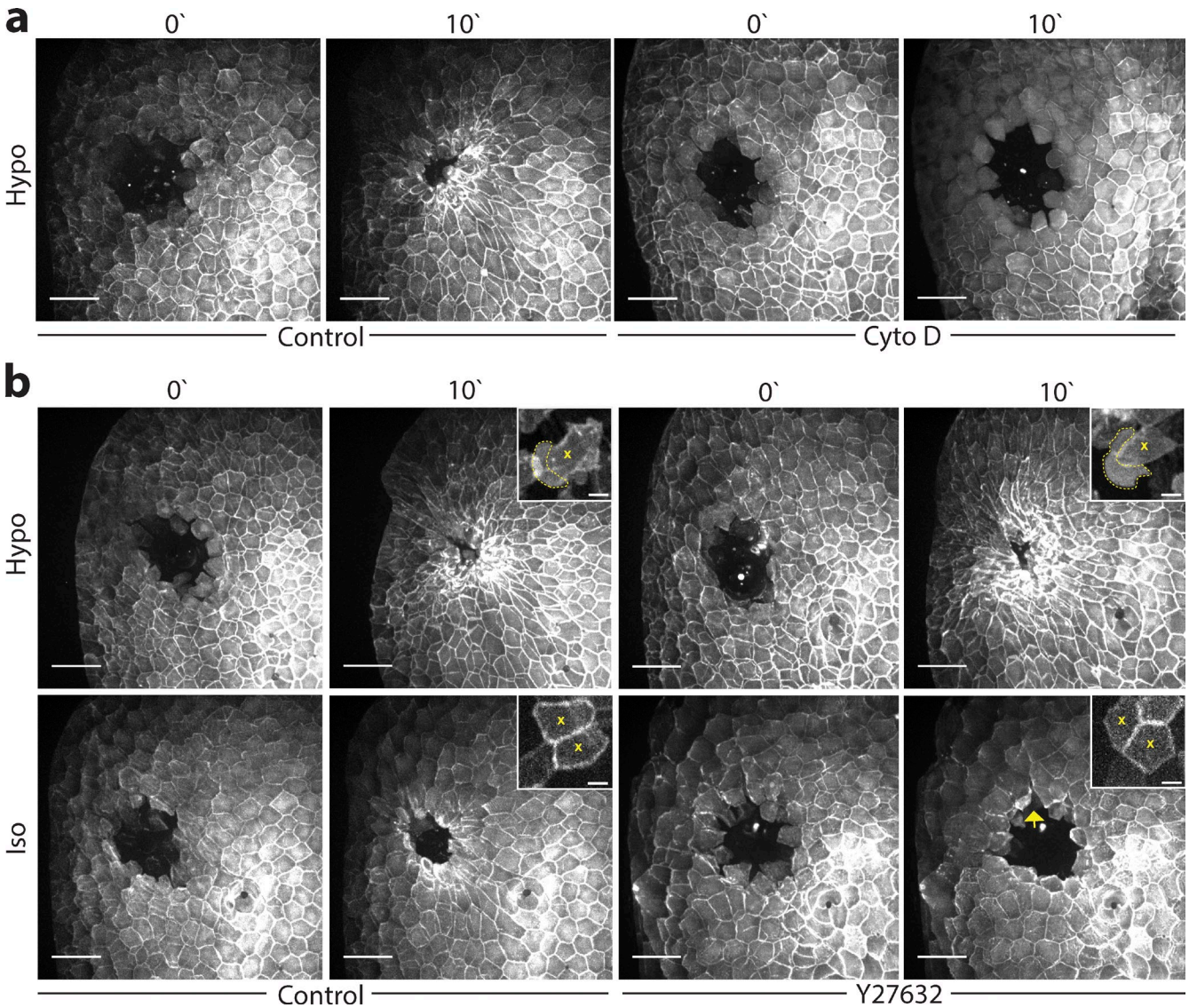

Figure S2. **Basal epithelial cell migration is the primary driving force behind rapid wound closure.** (a and b) Representative time-lapse images of 2.5–3 dpf *Tg(krt4:AKT-PH-GFP)* transgenic zebrafish larvae labeled exclusively in the suprabasal layer. Larvae were mounted in 1% low-melting-point hypotonic or isotonic agarose and UV laser wounded to produce round puncture wounds. (a) Larvae wounded in ±100 µM cytochalasin D, an inhibitor of actin dynamics. Note the complete inhibition of wound closure after 10 min compared with the control. Hypo controls in a and b were from the same dataset. (b) Larvae were wounded in either Hypo or Iso E3 medium with or without 100 µM Rho kinase (Y27632) inhibitor. (b, bottom) At 10 min after injury, both isotonic wounds fail to close in the absence of basal cell migration (insets), but wound margin contraction is additionally absent in isotonic samples treated with Y27632 (jagged margin; yellow arrow), in comparison to iso control (rounded wound margin). (b, top) In the presence of hypotonically induced basal cell lamellipodial migration (insets), both hypo Y27632 and hypo control samples exhibit substantial wound closure by 10 min. See also Video 5. All insets capture representative AKT-PH-mKate2 mosaically labeled basal cells (4–8-cell mRNA injections) from independent samples under identical treatments as the larger images. Inset images were captured at 2.5 min after wounding, and at similar distances from the wound (~100 µm); lamellipodia are delimited with yellow broken lines, and cell bodies are marked with a yellow x. Representative images of at least $n = 3$ larvae are shown. Some representative panels are from the same dataset used to quantify wound closure in Fig. 1. Bars: (main panels) 50 µm; (insets), 10 µm.

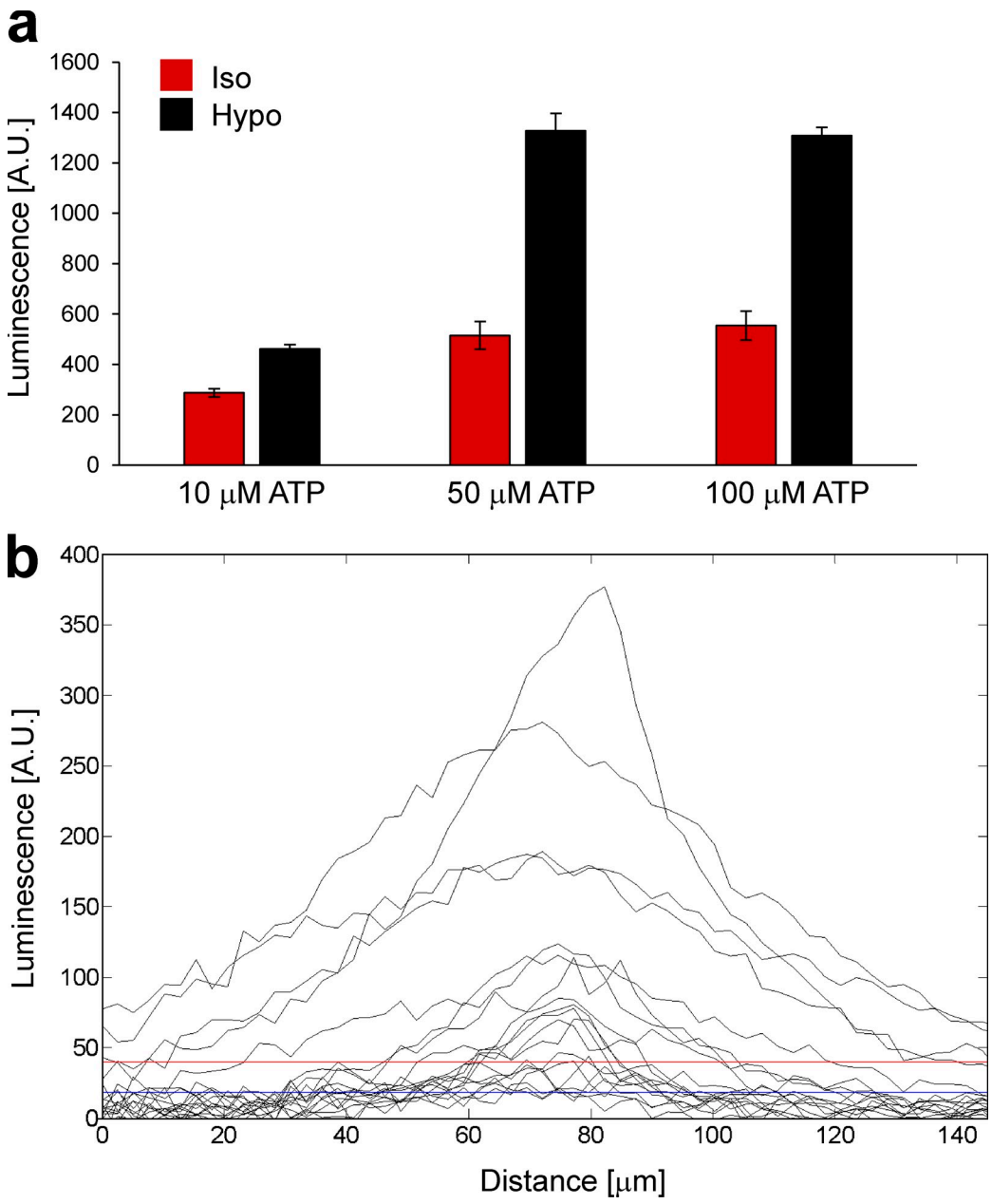

Figure S3. **The effect of tonicity on light generation by firefly luciferase.** (a) Mean luminescence of hypotonic (5 mM NaCl) or isotonic (145 mM NaCl) E3 solutions at the indicated concentrations of ATP (for details see Materials and methods). On average, luminescence is quenched approximately twofold in isotonic solutions. Error bars indicate standard deviation (n = 3 technical replicates). (b) Isotonic quenching of luminescence cannot account for lack of ATP signal detection during isotonic incubation of wounded fish. Profile plots of all detectable luminescence signals in a typical in vivo luminescence experiment are shown. The intensity measurements were performed on one representative sample from the dataset depicted in Fig. 5. Black lines, profile plots centered on signal maximum (profile thickness = 10 pixels). Blue line, detection limit as defined as five times the standard deviation of baseline noise. Red line, quenching threshold as defined as detection limit multiplied with the quenching factor determined in a. Signals above the quenching threshold should be detectable in our assay regardless of the tonicity of the medium.

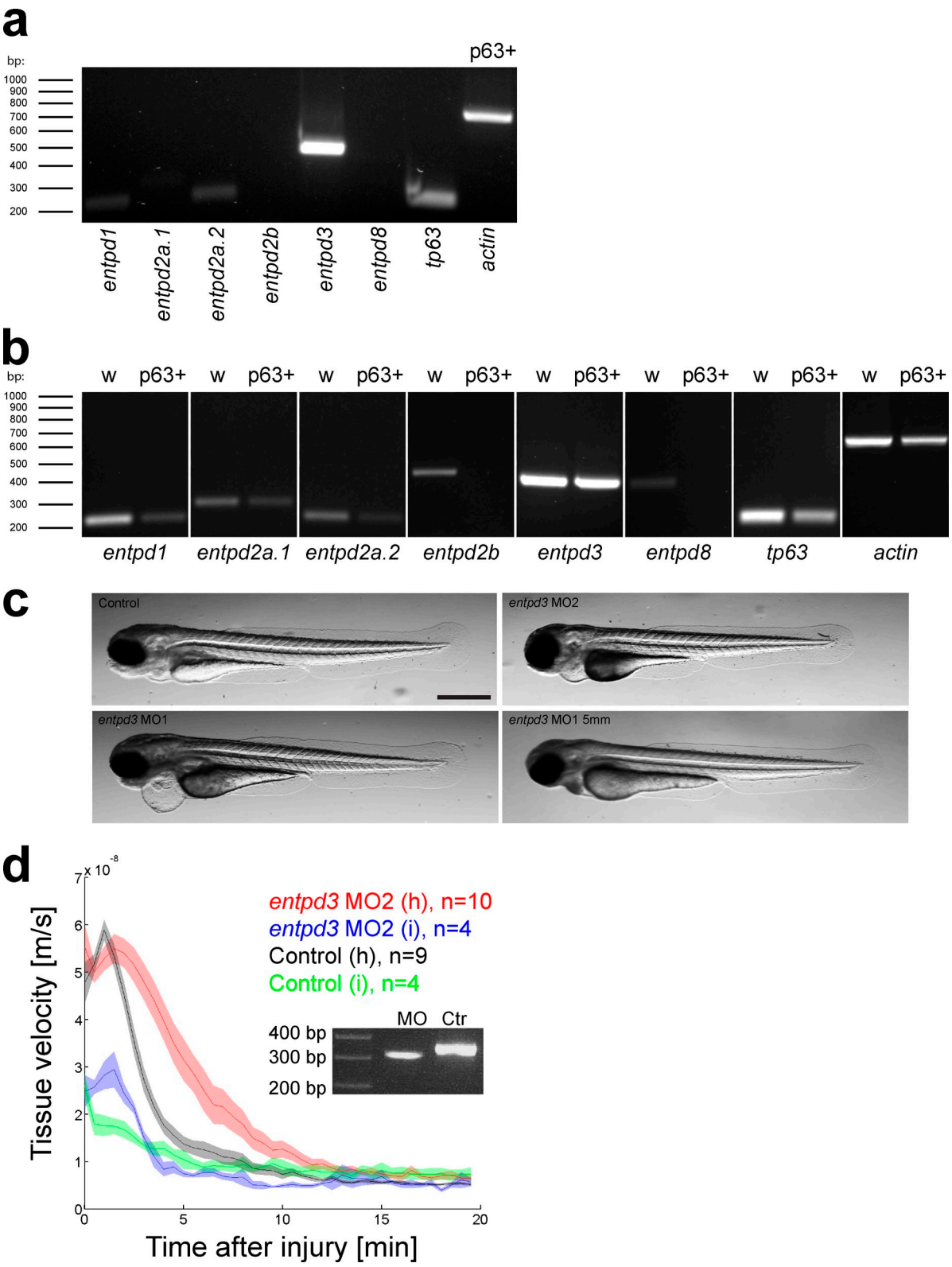

Figure S4. ***entpd3* is the predominant ecto-NTP diphosphohydrolase (ENTPD/NTPDase) in the zebrafish epidermis, and regulates tissue velocity during wound closure.** Epidermal mRNA was isolated by dissociating and FACS sorting 2.5–3-dpf transgenic zebrafish expressing GFP in basal cells via *Tg(ΔNp63:Gal4;UAS:GFP)* (Materials and method section). (a) mRNA levels were compared between known extracellular NPTDases using semiquantitative RT-PCR, where the strongest detectable mRNA expression in the epidermis was exhibited by *entpd3*. Note the expression of the epidermal-enriched *tp63* transcript. (b) For each primer set, PCR cycle number was adjusted to reveal the relative abundance of each *entpd* in the tp63-positive (p63+) sorted population relative to mRNA levels present in whole larvae (w; Materials and methods section). Note, the separation of panels in b indicates independent PCR experiments. Panels in a and b are representative of $n = 2$ independent sorting experiments. (c) Representative whole images of 2.3–3-dpf *Tg(krt4:AKT-PH-GFP) entpd3* morphants. Top left, control; top right, splice-blocking morphant MO2 (~19 ng); bottom left, translation-blocking MO1 morphant (~19 ng); bottom right, translation-blocking MO1 five-nucleotide mismatch control morphant MO1 5 mm (~19 ng). Bar, 500 μm. (d) Global PIV analysis of the indicated number of *Tg(krt4:AKT-PH-GFP)* larvae subjected to UV-laser-cut injury in Hypo or Iso medium, with or without splice-blocking morpholino-mediated knockdown of *entpd3* (*entpd3* MO2, ~19 ng). (Inset) RT-PCR of *entpd3* MO2 knockdown; note the downshift associated with aberrant splicing and nucleotide deletion in the entpd3 coding sequence (see Materials and methods).

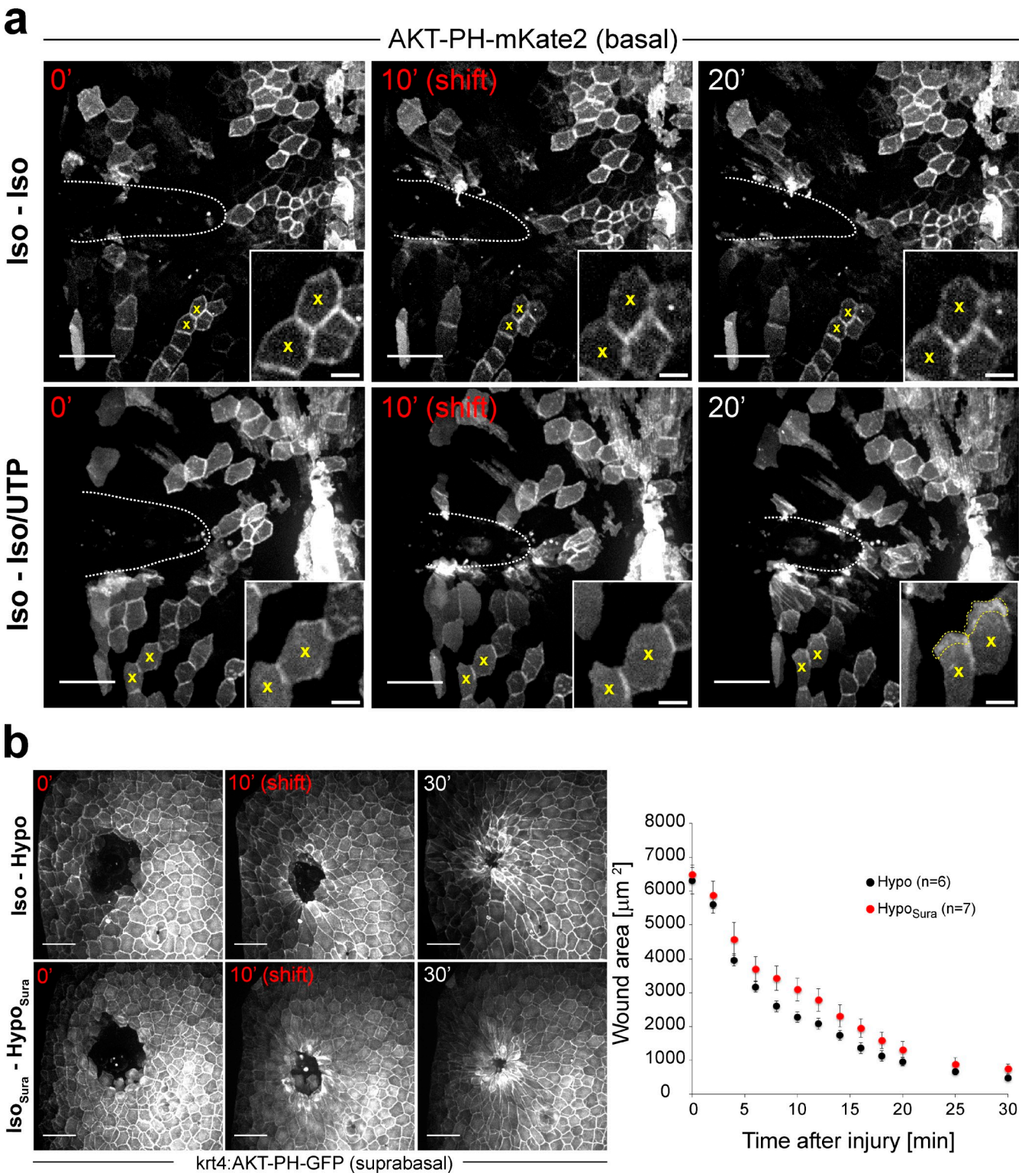

Figure S5. **UTP reconstitutes basal cell migration, and suramin fails to inhibit hypotonic wound closure.** (a) Representative time-lapse images of 2.5–3-dpf zebrafish larvae exhibiting mosaic membrane labeling in predominantly the basal layer by injection of mRNA encoding AKT-PH-mKate2 into the yolk of 4–8-cell stage embryos. Larvae were mounted in 1% low-melting-point isotonic agarose. After a 10-min incubation in isotonic E3 medium (red time indices), mounted larvae were covered with a bolus (~10× agarose volume equivalent) of isotonic E3 ± 5 mM UTP. Yellow x, representative morphological response after addition of isotonic solution ± 5 mM UTP. Note the lamellipodial protrusions that developed shortly after UTP addition (yellow broken line). See also Video 10. Representative iso-iso control sample and dataset were also used for ATP experiment shown in Fig. 7 a. (b) Time-lapse images of 2.5–3-dpf larvae puncture-wounded with a UV laser in Iso medium containing 1% low-melting-point agarose in the presence or absence of 1 mM suramin (nonselective P2 receptor antagonist). After a 10-min incubation to permit suramin infusion into the wound (red time indices), an ~10× bolus of hypotonic E3 ± 1 mM Suramin was added to the sample. (Right) Wound area quantification as a function of time after injury. Error bars indicate SEM of the indicated (*n*) number of larvae. Bars: (a, main panels, and b) 50 µm; (a, insets) 10 µm.

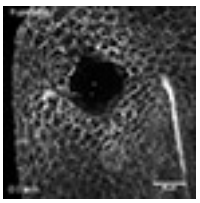

Video 1. **Isotonicity inhibits rapid wound closure in the larval zebrafish tail fin.** 2.5–3-dpf zebrafish tail fins expressing GFP-Utr-CH were UV-laser-wounded in hypotonic, isotonic (NaCl), or isotonic (sucrose) E3 medium. Images were acquired by time-lapse spinning disk confocal microscopy (Eclipse FN1; Nikon). Imaging begins ∼0.5–1 min after wounding. Frames were taken every 30 s. Video stills are in Fig. 1 b. Bar, 50 µm.

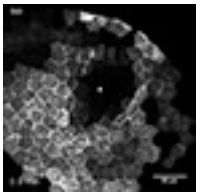

Video 2. **Isotonic inhibition of rapid wound closure is reversible.** 2.5–3-dpf zebrafish tail fins expressing AKT-PH-GFP in the suprabasal epidermal layer (*krt4* promoter) were UV-laser-wounded in isotonic (NaCl) medium and shifted after 40 min into hypotonic E3 medium. Images were acquired by time-lapse spinning disk confocal microscopy (Eclipse FN1; Nikon). Imaging begins ∼0.5–1 min after wounding. Frames were taken every 30 s. Video stills are in Fig. 1 c. Bar, 50 µm.

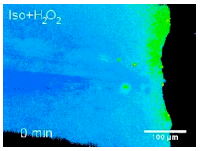

Video 3. **Hypotonicity triggers rapid barrier recovery of the wounded tail fin epidermis.** 2.5–3-dpf transgenic *Tg(actb2:HyPer)* larval tail fins amputated in isotonic (NaCl) medium and shifted into hypotonic or isotonic medium supplemented with 1 mM H_2O_2. Images were acquired by time-lapse epifluorescence microscopy (Eclipse Ti; Nikon). H_2O_2 shifting and imaging starts 1 h after wounding. Frames were taken every minute. Color-coded HyPer ratios (E_{500}/E_{420}) are depicted. Red, high [H_2O_2]. Blue, low [H_2O_2]. Video stills are in Fig. 1 d. Bar, 100 µm.

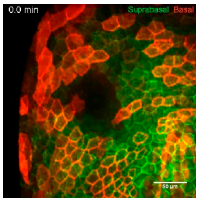

Video 4. **Distinct wound responses in the bilayered tail fin epidermis.** 2.5–3-dpf UV-laser-wounded zebrafish tail fins displaying individually labeled suprabasal (green, *Tg(krt4:AKT-PH-GFP)*) and basal (red, AKT-PH-mKate2 mRNA-injected) cell layers wounded in normal hypotonic E3 medium. Images were acquired by time-lapse spinning disk confocal microscopy (Eclipse FN1; Nikon). Frames were taken every 30 s. Imaging begins ∼0.5–1 min after wounding. The video is representative of $n = 4$. Video stills are in Fig. 2 a. Bars, 50 µm.

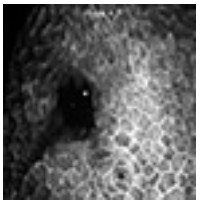

Video 5. **The effect of Rho-kinase inhibition on wound closure.** 2.5–3-dpf *Tg(krt4:AKT-PH-GFP)* zebrafish tail fins expressing AKT-PH-GFP in the suprabasal epidermal layer were UV-laser-wounded in hypotonic medium in the presence/absence of Rho kinase inhibitor (Y = Y27632, 100 µM). Frames were taken every 30 s. Imaging begins ∼0.5–1 min after wounding. The video is representative of $n = 5$. Video stills from the same dataset are in Fig. S2 b. Bar, 50 µm.

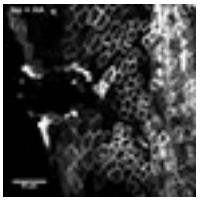

Video 6. **Arachidonic acid does not reconstitute directional cell migration after isotonic injury.** 2.5–3-dpf zebrafish tail fins expressing AKT-PH-mKate2 in basal cells (AKT-PH-mKate2 mRNA injected), UV-wounded in isotonic (NaCl) medium, and then shifted to isotonic medium ± 10 µM arachidonic acid (AA). Shifting occurs at ∼10 min. Images were acquired by time-lapse spinning disk confocal microscopy (Eclipse FN1; Nikon). Frames were taken every 30 s. Imaging begins ∼0.5–1 min after wounding. The video is representative of $n = 3$ different larvae. Bar, 50 µm.

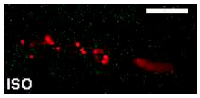

Video 7. **Hypotonic medium triggers ATP release at wounded tail fins.** Luciferase/luciferin luminescence imaging of 2.5–3-dpf wt larval tail fins subjected to tip amputation in isotonic (NaCl) medium, and shifted to hypotonic medium after 20 min. Green, ATP-dependent luminescence. Red, staining of damaged cells by SYTOX Orange. Images were acquired by time-lapse epifluorescence microscopy (Eclipse Ti; Nikon). Frames were taken every 40 s. Imaging begins ∼3 min after wounding. The video is representative of *n* = 6 different larvae. Video stills are in Fig. 5 a. Bars, 100 µm.

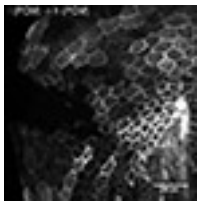

Video 8. **Pharmacologic inhibition of ENTPDases and broad-spectrum inhibition of ecto-ATPase enhances basal cell migration.** 2.5–3-dpf UV-laser-wounded zebrafish tail fins expressing AKT-PH-mKate2 in basal cells wounded in isotonic (NaCl) medium with 100 µM POM/compound 7 inhibitor, and then shifted to hypotonic medium with 100 µM POM (center), or wounded in isotonic (NaCl) medium with 5 mM ATPγS, and then shifted to hypotonic medium with 5 mM ATPγS (right). Isotonic to hypotonic control is shown (left). Shifting occurs at ∼10 min. Images were acquired by time-lapse spinning disk confocal microscopy (Eclipse FN1; Nikon). Frames were taken every 30 s. Imaging starts ∼0.5–1 min after wounding. Rigid body registration was performed (Fiji). Responses are representative for at least *n* = 3 different larvae. Bar, 50 µm.

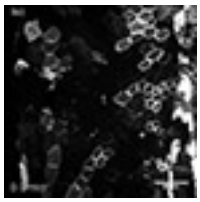

Video 9. **ATP, but not stabilized analogues or hydrolysis products of ATP, reconstitutes basal epithelial cell migration to the wound in isotonic medium.** A composite movie of 2.5–3-dpf zebrafish tail fins expressing AKT-PH-mKate2 in basal cells and UV-laser-wounded in isotonic (NaCl) medium, then shifted to isotonic medium containing 5 mM of indicated compounds. Samples were shifted after ∼10 min. (left) Looped isotonic control movie for comparison. (right) Basal cell responses to ATP, Apyrase-treated ATP, ATPγS, Bz-ATP, ADP, ADPβS, AMP, and adenosine. Images were acquired by time-lapse spinning disk confocal microscopy (Eclipse FN1; Nikon). Frames were taken every 30 s. Imaging begins at ∼0.5–1 min after wounding. Video stills are in Fig. 7 a. The isotonic control is identical in Videos 9 and 10. Responses are representative for at least *n* = 3 different larvae. Bars, 50 µm.

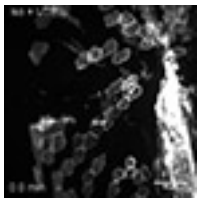

Video 10. **UTP, but not stabilized analogues or hydrolysis products of UTP, reconstitutes basal epithelial cell migration to the wound in isotonic medium.** A composite movie of 2.5–3-dpf zebrafish tail fins expressing AKT-PH-mKate2 in basal cells and UV laser wounded in isotonic (NaCl) medium, then shifted to isotonic medium containing 5 mM of the indicated compounds. Samples were shifted after ∼10 min. (left) Looped isotonic control movie for comparison. (right) Basal cell responses to UTP, UTPγS, UDP, 3-phenacyl UDP, UDP glucose, UMP, and Uridine. Images were acquired by time-lapse spinning disk confocal microscopy (Eclipse FN1; Nikon). Frames were taken every 30 s. Imaging begins at ∼0.5–1 min after wounding. Video stills are in Fig. S5 a. The isotonic control is identical in Videos 9 and 10. Responses are representative for at least *n* = 3 different larvae, except for 3-phenacyl UDP (*n* = 2). Bars, 50 µm.

Table S1. **Pharmacological agonist profile of known P2 receptors**

Agonist	Receptor
ATP[a]	P2Y1, P2Y2, P2Y4, P2Y11, P2Y12,P2Y13, P2X1, P2X2, P2X3, P2X4, P2X5, P2X6, P2X7
ADP[b]	P2Y1, P2Y6, P2Y12, P2Y13
AMP[b]	A1
A[b]	A1, A2A, A2B, A3
UTP[a]	P2Y2, P2Y4, P2Y6
UDP[b]	P2Y6, P2Y14
ATPγS[b]	P2Y1, P2Y2, P2Y11, P2Y13, P2X2, P2X5
BzATP[b]	P2X1, P2X3, P2X7
ADPβS[b]	P2Y1, P2Y11, P2Y12, P2Y13
UTPγS[b]	P2Y2, P2Y4
3-PA-UDP[b]	P2Y6
UDP-Gluc[b]	P2Y14

Underlining indicates P2 receptors that respond to both ATP and UTP. Main source: IUPHAR/BPS. ATP, Adenosine 5′-triphosphate; ADP, adenosine 5′-diphosphate; AMP, adenosine 5′-monophosphate; A, adenosine; UTP, uridine 5′-triphosphate; UDP, uridine 5′-diphosphate; ATPγS, adenosine 5′-[γ-thio] triphosphate; Bz-ATP, 2′(3′)-*O*-[4-Benzoylbenzoyl]-adenosine 5′-triphosphate; ADPβS, adenosine 5′-[β-thio]-diphosphate; UTPγS, uridine 5′-[γ-thio]-triphosphate; 3-PA-UDP, 3-[2-Oxo-2-phenylethyl]-uridine-5′-diphosphate; UDP-glucose, uridine 5′-diphosphoglucose.
[a]Ligand elicits migration response.
[b]Ligand elicits no migration response.